ORIGINAL

Evaluation of heat transfer surfaces for compact recuperator using a CFD code

T. P. Ashok Babu · Mohammad Shekoor Talekala

Abstract Exhaust recovery recuperator is mandatory in order to realize a thermal efficiency of 30% or higher for micro turbines. In this work an attempt is made to select the cross corrugated heat transfer surface with minimum core volume of a recuperator matrix using a CFD code. Analysis is carried out for selected cross corrugated heat transfer surface configurations. The relation between the minimum core volume from design calculation and average skin friction coefficient from CFD analysis has been established.

List of symbols

A_d	heat transfer area (m^2)
A_{front}	frontal area of representative recuperator (m^2)
A_{total}	total heat transfer area of representative recuperator (m^2)
CC	cross corrugated heat transfer surface, also called chevron pattern
C	coefficient of compactness, ratio of heat transfer surface/internal volume (m^2 m^{-3})
D_e	equivalent diameter, $4V/A_d$ (m)
D_h	hydraulic diameter (m)
f	Fanning friction factor
H_i	internal height (mm)
h	convective heat transfer coefficient (W m^{-2} K^{-1})
j	Colburn factor $St*Pr^{2/3}$
k	thermal conductivity (W m^{-1} K^{-1})
$L_{recuperator}$	length of recuperator matrix (m)
$\dot{m}$	mass flow rate (kg s^{-1})
Nu	Nusselt number
p	pressure (N m^{-2})
P	pitch of corrugation (mm)
ΔP	pressure drop (N m^{-2})
P/H_i	aspect ratio
Pr	Prandtl number
q	heat transfer rate (W)
Re	Reynolds number
S	thickness of the corrugated surface (mm)
St	Stanton number
T_f	bulk temperature of the fluid (K)
T_w	mean temperature of the middle wall (K)
ΔT_{log}	log mean temperature difference
U	over all heat transfer coefficient (W m^{-2} K^{-1})
V	volume flow rate (m^3 s^{-1})
$V_{recuperator}$	internal volume of representative recuperator (m^3)
W	velocity (m s^{-1})
W_{av}	average velocity of fluid (m s^{-1})
v	kinematic viscosity (m^2 s^{-1})
θ	included angle between corrugations (°)
λ	fluid thermal conductivity (W m^{-1} K^{-1})
μ	dynamic viscosity (kg m^{-1} s^{-1})
ρ	density (kg m^{-3})

T. P. Ashok Babu · M. S. Talekala (✉)
Mechanical Engineering Department, National Institute of
Technology Karnataka, Surathkal 575025, Karnataka, India
e-mail: shek117@rediffmail.com

T. P. Ashok Babu
e-mail: tpashok@gmail.com

1 Introduction

The use of exhaust heat recovery exchangers has always been an option for improving efficiency, and they are applicable in principle to a wide range of gas turbine applications.

Nevertheless, recuperators have found only limited acceptance because of their earlier bulky size, poor reliability and high cost. To date the use of a recuperator has been essentially a user option, but there is now an emerging engine application, namely micro turbines, where its use is mandatory to achieve engine efficiencies of 30% and higher [1].

The demand for small scale flexible and ecological energy production is globally growing. One interesting alternative is a high speed micro gas turbine plant for combined electrical power and heat generation. Uechi et al. [2] have showed that one of the most important technical issues for improving the plant efficiency is to enhance the effectiveness of the recuperator.

The paramount requirements for the recuperator are low cost and high effectiveness. These characteristics must be accomplished with a heat exchanger that has good reliability, high performance potential, compact size, light weight, proven structural integrity, and adaptability to automated high volume production methods.

Literature reveals that compact recuperators with cross corrugated plates are widely recommended for Micro turbines. Utriainen and Sunden [3] conclude that the recuperator with the cross corrugated surfaces show superior performance over the others giving a small volume and weight of the heat transfer matrix, and probably is easier to manufacture with small passage dimensions.

Minimizing the recuperator size is essential for the compactness of the micro turbines. This work is a small step towards the goal of establishing a compact and cost-effective recuperator for the new class of very small gas turbines that are close to entering service.

1.1 The cross corrugated (CC) surface

The CC surface, see Fig. 1, used in recuperators has duct diameter much smaller than 5 mm and as it fulfills all requirements of a primary surface, it may be considered as a primary surface.
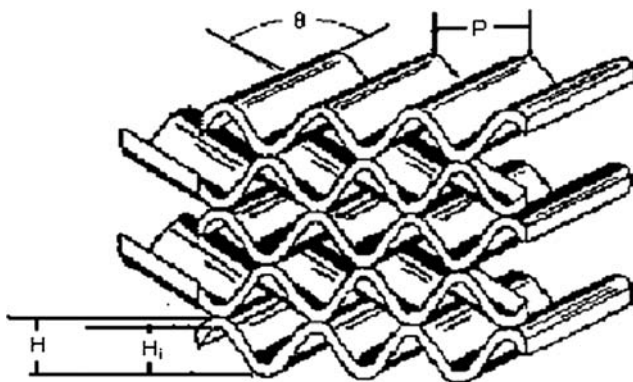

Fig. 1 Cross corrugated surface

Even though there are several investigations of the CC surface performance in the literature, they provided no detailed data about CC geometry studied. Heavner et al. [4] proposed a theoretical approach, supported by experimental data, to predict heat transfer coefficients of cross corrugated (chevron) type plate heat exchangers. They report the dependence of the included angle (θ) on CC surface performance, but all other geometrical details of the CC surfaces are missing. Focke et al. [5] reported experimental work in the Reynolds number range 100–60,000, included angles 0–180° and P/H_i = 2. Muley and Manglik [6] report experimental results for the Reynolds number range 400–9,000, included angle 60–120° and P/H_i = 3.6. Muley and Manglik [7] report experimental results for the Reynolds number range 2–350, included angle 60–120° and P/H_i = 3.6.

Stasiek et al. [8] and Ciofalo et al. [9], performed a systematic investigation on the fluid flow and heat transfer characteristics by means of experimental and numerical methods. Predictions of thermal and hydraulic performance in the Reynolds number range 500–10,000, included angle 30–150° and P/H_i range 2–4 were presented in their report. Their investigation is also one of the few papers reporting thermal performance for experiments using air as the working fluid. Utriainen and Sunden [3] reported review studies and design calculation results for CC surfaces for 50 KW recuperator, in the Reynolds number range 274–529, included angle 45–75° and P/H_i range 2.2–4. Data of the thermal and hydraulic performance used for design calculations in the present study have been retrieved from the work by Utriainen and Sunden [3].

Despite all the previous efforts, to the author's knowledge, the numerical investigations of flow and heat transfer, for CC surface are a few, and a few numerical simulations available adopted periodic boundary conditions in the inlet/outlet faces. There are no studies on using CFD simulations for selection of heat transfer surface with minimum core volume of recuperator matrix.

The aim of this work is to provide information on how CFD studies may be used to narrow down our search on heat transfer surface configuration which results in minimum core volume of recuperator matrix.

However experiments are still necessary in order to validate and calibrate models and numerical methods, and a complete picture of flow and heat transfer in the exchanger passages can only be given by parallel experiments and computational studies.

In this study the cross corrugated surfaces, CC 2.2–60, CC 2.2–75, CC 3.1–60, CC 4–45 for which experimental data's available in Utriainen and Sunden [3] are selected for establishing the relation between the minimum core volume from design calculation and average skin friction coefficient from CFD analysis. Design calculations of a

recuperator matrix for a 10 kW micro turbine have been carried out for the selected surfaces with the assistance of experimental data's available in Utriainen and Sunden [3]. The presented results of the design calculation are focused on recuperator core. CFD analysis also is carried out for the same surfaces as an effort to establish the relation between the minimum core volume from design calculation and average skin friction coefficient from CFD analysis. The study is carried out for Air and Argon as heat transfer fluid which exhibit similar nature of relation between the minimum core volume from design calculation and average skin friction coefficient from CFD analysis.

The model is validated using limited experimental results available in Jixiang et al. [10] and Utriainen and Sunden [3], which exhibits a satisfactory agreement considering the gap between corrugated plates, indicating the validity of the present computation method.

2 Design calculations

A preferred way to compare different surfaces for a recuperator is to carry out recuperator design calculations and to compare, e.g., physical size, weight, etc. In this paper, recuperator heat transfer matrix calculations see the Appendix; have been carried out for a representative micro turbine having an output power of 10 kW. Some selected surfaces given in Table 1 are used for the calculation. Operating conditions of micro turbine recuperator are given in Table 2.

In the calculations, some assumptions, based on experience from the industry, have been made:

- Ninety percent of the total heat is transferred in the heat transfer matrix.
- Sixty percent of the total pressure drop is over the heat transfer matrix, All primary surface variants are suitable for the same kind of recuperator design, i.e., the pressure drop of the inlet and outlet manifolds may be regarded as equal for all surface variants.
- The metal sheet thickness is 0.08 mm.
- The hydraulic diameter is 1.54 mm for both the hot and cold sides of the recuperator matrix.

Table 1 Geometrical data of surfaces

Surface	Pitch P (mm)	Int. height H_i (mm)	P/H_i	C (m² m⁻³)	θ (°)
CC 2.2–60	2.36	1.07	2.22	1,298	60
CC 2.2–75	2.36	1.07	2.22	1,298	75
CC 3.1–60	2.86	0.93	3.06	1,298	60
CC 4–45	3.48	0.87	4.0	1,299	45

Table 2 Micro turbine recuperators operating condition

Hot fluid	Air
Inlet temperature of hot fluid	955 K
Mass flow rate of hot fluid	0.1289 kg s⁻¹
Inlet pressure of hot fluid	10 bar
Cold fluid	Air
Inlet temperature of cold fluid	432 K
Mass flow rate of cold fluid	0.1279 kg s⁻¹
Inlet pressure of cold fluid	3 bar

Stainless steel is selected as recuperator material since it suits our following operating condition.

Compressor pressure ratio = 3.
Hot gas inlet temperature = 682°C.

In Table 3 the resulting recuperator matrix volume of each surface for air and argon as fluids are shown. The CC surfaces having the smallest P/H_i ratios result in the smallest matrix volumes. Similarly, high values of the corrugation angle θ give smaller volumes due to better thermal performance but the higher pressure drop necessitate shorter length of the matrix.

Design results for air are compared with volume goodness diagram and area goodness diagram. The first one is the volume goodness factor comparison; see Fig. 2, where the axes represent the heat transfer coefficient, h, and pumping power per unit heat transfer area $\Delta P \, V/A_d$, respectively. ΔP is pressure drop along the duct, V is the volume flow rate and A_d is the heat transfer surface area. A high position in this plot indicates a small volume of the recuperator core but it does not say anything of the shape of the volume. In the volume goodness factor diagram an

Table 3 Results of design calculations

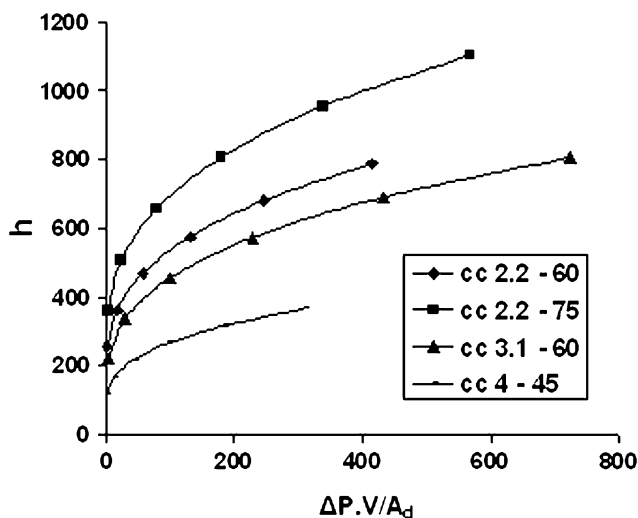| Configuration	Reynolds no		Frontal area (m²)		Length (m)		Volume (m³)		Pressure drop (%)	
	Air	Argon	Air	Argon	Air	Argon	Air	Argon	Air	Argon
CC 2.2–60	534	757	0.0226	0.0125	0.0873	0.1123	0.001972	0.00141	0.029	0.029
CC 2.2–75	534	766	0.0226	0.0124	0.0623	0.0806	0.001409	0.00100	0.029	0.029
CC 3.1–60	349	552	0.0346	0.0173	0.0894	0.1020	0.003089	0.00176	0.029	0.029
CC 4–45	414	584	0.0291	0.0163	0.1674	0.2198	0.004880	0.00358	0.029	0.029

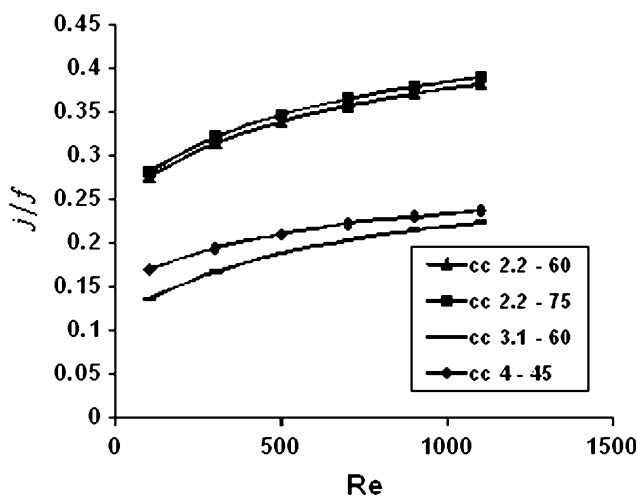Fig. 2 The volume goodness diagram for air

Fig. 3 The area goodness diagram for air

equal hydraulic diameter for all surface variants is required for correct comparison. The second plot, see Fig. 3, shows the performance of the surfaces in a diagram for flow area goodness factor comparison where the ratio of the Colburn factor and the Fanning friction factor (j/f) is plotted versus the Reynolds number Re. A high position in this plot indicates a small flow area of the recuperator. Combining these two diagrams gives an opportunity to find surfaces giving small physical recuperator size but also means to avoid very flat recuperators, i.e., large frontal area but small length in the flow direction.

3 Study of simplified geometry

In the present study effort is made to analyze the performances of compact heat exchanger surface comprising of

corrugated walls with herringbone design, using a CFD code namely FLUENT 6.1 developed by Fluent technologies.

Decide the type of flow in such narrow passages is still an open issue in the literature. Shah and Wanniarachchi [11] declare that, for the Reynolds number range 100–1,500, there is evidence that the flow is already turbulent, a statement that is also supported by Vlasogiannis et al. [12], whose experiments in a plate heat exchanger verify that the flow is turbulent for $Re > 650$. Lioumbas et al. [13], who studied experimentally the flow in narrow passages during counter-current gas–liquid flow, suggest that the flow exhibits the basic features of turbulent flow even for the relatively low gas Reynolds numbers tested ($500 < Re < 1,200$). Focke and Knibbe [14] performed flow visualization experiments in narrow passages with corrugated walls. They concluded that the flow patterns in such geometries are complex, due to the existence of secondary swirling motions along the furrows of their test section and suggest that the local flow structure controls the heat transfer process in such narrow passage.

The choice of the most appropriate turbulence model for CFD simulation is another open issue in the literature. The most common two-equation model, based on the equations for the turbulence energy k and its dissipation ε, is the $k - \varepsilon$ model. Ciofalo et al. [9] state that the standard $k - \varepsilon$ model using 'wall functions' over predicts both wall shear stress and wall heat flux, especially for the lower range of the Reynolds number encountered in this kind of equipment. Menter and Esch [15] note that the over prediction of heat transfer is caused by the over prediction of turbulent length scale in the region of flow reattachment, which is a characteristic phenomenon appearing on the corrugated surfaces in these geometries. An alternative to the $k - \varepsilon$ model is the $k - \omega$ model developed by Wilcox. The $k - \omega$ model, which uses the turbulence frequency ω in place of turbulence dissipation ε, appears to be more robust, even for complex applications, and does not require very fine grid near the wall. The main disadvantage of $k - \omega$ model is its sensitivity to the free stream values of turbulence frequency ω outside the boundary layer, which affects the solution and, in order to avoid this, a combination of the two models, $k - \varepsilon$ and $k - \omega$, i.e., the shear-stress transport (SST) model is proposed (Menter and Esch [15]). The SST model can switch automatically between the two aforementioned turbulence models using specific 'blending functions' that activate the $k - \omega$ model near the wall and the $k - \varepsilon$ model for the rest of the flow. Although the SST model combines the most widely used two-equation turbulence-models, other models, like large-Eddy simulation (LES) is considered more appropriate in turbulent flow simulation. However, the LES model is considered less robust and requires high-computational power.

Table 4 Geometric parameters used for the model

Plate length	0.062 m
Plate width	0.010 m
Distance between the crest	0.0001 m

In the present study the SST turbulence model is preferred over other flow models for simulations. This simple model, comprised of three corrugated plates having their crest nearly in contact, with hot and cold fluids flow alternately through passage created between the plates. Plate length of 62 mm is used for all the surfaces. Geometric parameters used for the model is given in Table 4. Analysis is carried out for air and argon as heat transfer fluid. Mass flow rate at inlet and pressure at outlet is used as the boundary condition. Same mass flow rate at inlet is applied for all the surfaces.

3.1 Grid generation

The computation domain of the model is covered with unstructured tet/hybrid grids. The commercial code GAMBIT has been selected to generate these grids due to its excellent merit of managing very complex 3D geometries. Grid interval size of 0.2 is selected. Depending on the intersection angle between corrugated plate and shape factor (pitch, height) grid cells in the range of 1,52,687–1,68,408 are used to discretize the computation domain.

3.2 Grid independency check

Grid independency check has been conducted to avoid the numerical error due to dependency of results on grid sizes. The results of Grid independency check is shown in Fig. 4. Course grid refer to a grid size of 0.4, fine grid refer to a grid size of 0.3 and finer grid refer to a grid size of 0.2.

3.3 Numerical solution

The computer code FLUENT 6.1 developed by Fluent technologies and based on a finite volume technique is used for three-dimensional numerical simulations of the fluid flow and heat transfer. The discretization schemes of convective terms in momentum and energy equations adopt QUICK scheme with three-order precision. The SIMPLEC pressure-velocity coupling algorithm is used here. For all reported calculation results, the convergence criteria are the convergence residuals less than 10^{-3} for velocity equations and less than 10^{-6} for energy equations. The convergence became more and more difficult for these geometry channels whose intersection angles are larger or smaller.
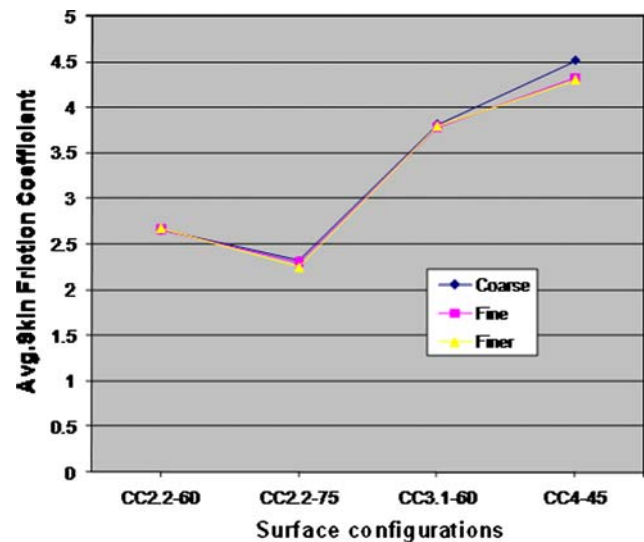
Fig. 4 Grid independency plot with air as fluid

4 Performance parameters and model validation

In heat exchanger design, the most relevant performance parameters are pressure drop and heat transfer rate. It is desirable that high heat transfer rates are obtained while pressure losses are as low as possible. The pressure losses are evaluated using dimensionless pressure gradient per unit length along the mainstream direction, and the defining equation is as follows:

Friction factor

$$f = \frac{\Delta P D_{\mathrm{e}}}{2\rho \Delta L W_{\mathrm{av}}^2}. \tag{1}$$

Heat transfer can be described by a dimensionless parameter Nusselt number. The surface-weighted averaged heat transfer rates can be defined by:

Nusselt number

$$Nu = \frac{q_{\mathrm{w}} D_{\mathrm{e}}}{\lambda (T_{\mathrm{w}} - T_{\mathrm{f}})} \tag{2}$$

To the best of author's knowledge, experimental values of heat transfer and pressure drop are very limited in the open literature for the corrugated plate geometry, since these data are proprietary. The present study confirms the validation of numerical code by comparing the numerical results predicted with the experimental results presented by Utriainen and Sunden [3] and method used for comparison by Jixiang et al. [10] for CC 2.2–75 geometry. Figures 5 and 6 illustrate the friction factor and Nusselt number variation with Reynolds number from CFD analysis and experimental results presented by Utriainen and Sunden [3]. In spite of difference in geometry (the gap between the crest of two alternate plates used in the CFD analysis)
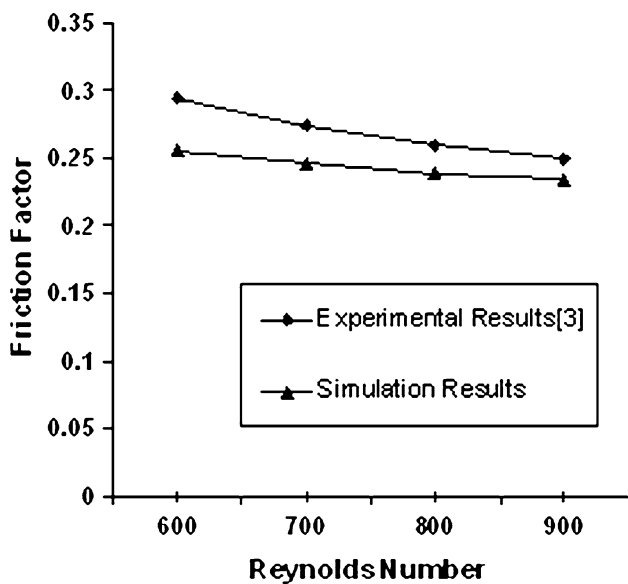
Fig. 5 Comparison between predicted and experimental results for fanning friction factor for CC 2.2–75 surface and the fluid is air
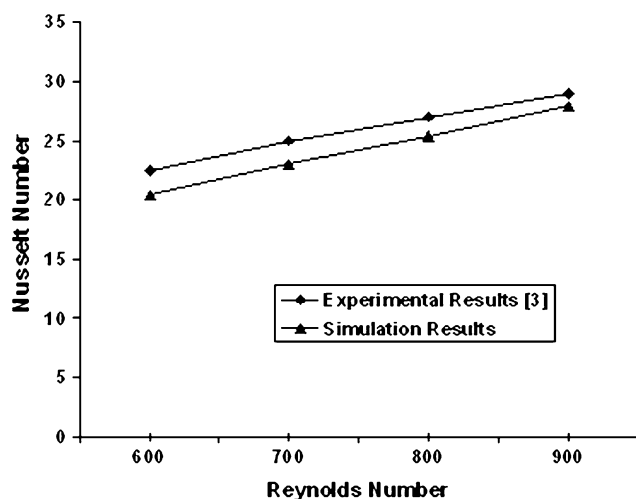

Fig. 6 Comparison between predicted and experimental results for average Nusselt number for CC 2.2–75 surface and the fluid is air

simulation results are in satisfactorily good agreement with the experimental results available, indicating the validity of the present computation method.

5 Results and discussion

The results presented in Table 5 indicate that average heat transfer coefficient increase with P/H_i ratio and decrease with corrugation angle θ for same size of the recuperator core and same flow condition.

The design calculation results and CFD analysis is compared with bar chart for volume of the recuperator matrix and average skin friction coefficients for the selected cross corrugated heat transfer surfaces. The first one is the bar chart for volume of the recuperator matrix, see Figs. 7 and 8, where the vertical axis represents the design calculation result of recuperator matrix volume. The second plot is the bar chart for average skin friction coefficients, see Figs. 9 and 10, where the vertical axis represents the CFD analysis result for average skin friction coefficients. The plots in Figs. 7 and 9, 8 and 10, indicates the relation between the results of design calculation for minimum core volume and results of CFD analysis for average skin friction coefficient. The surface with least recuperator matrix core volume is also seems to be with least average skin friction coefficient for separating wall. The increase of average skin friction coefficient indicates the requirement of increased core volume of the recuperator matrix. The authors carried out studies for Air and argon as heat transfer fluids which exhibit similar nature of relation between the minimum core volume from design calculation and average skin friction coefficient from CFD analysis.

The design calculation is possible with assistance of constants in Table 6 which is available through experimental studies. Therefore CFD analysis may be used to narrow down our search for heat transfer surfaces with minimum core volume of recuperator matrix.

6 Concluding remarks

The variation of main geometric details of cross corrugated surfaces (i.e., aspect ratio and angle of corrugation) makes it increasingly difficult to have a general design method. In the absence of adequate 'database' covering all possible configurations, it is nearly impossible to predict the highly
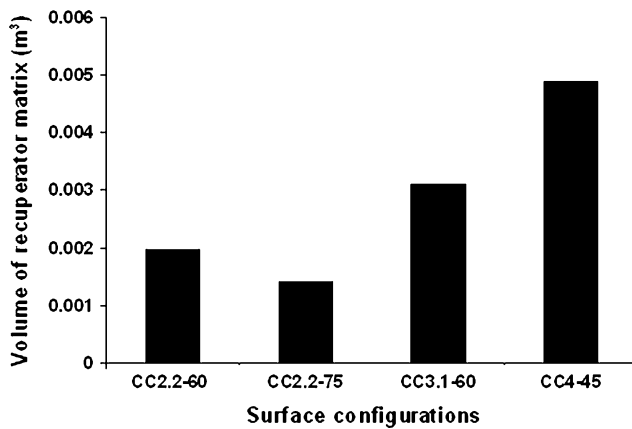
Table 5 Area weighted average results from CFD analysis	Configuration	Outlet temp. of cold fluid (K)		Heat transfer coefficient for the separating wall (w m^{-2} K^{-1})		Avg. skin friction coefficient for the separating wall	
		Air	Argon	Air	Argon	Air	Argon
	CC 2.2–60	750.32	752.36	130.37	65.64	2.68	2.74
	CC 2.2–75	737.25	743.09	120.05	60.23	2.25	2.32
	CC 3.1–60	756.85	759.39	148.55	75.91	3.80	4.18
	CC 4–45	758.66	765.09	158.03	82.29	4.31	6.01

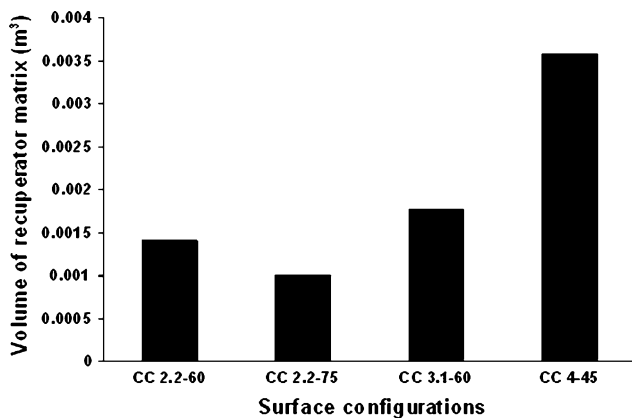**Fig. 7** Results of design calculation, volume of the recuperator matrix for air

Fig. 8 Results of design calculation, volume of the recuperator matrix for argon
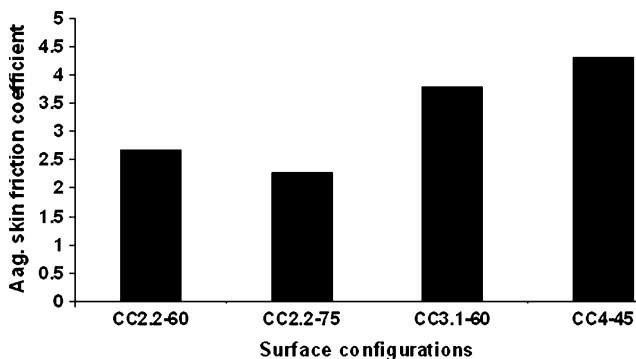

Fig. 9 Results of CFD analysis, average skin friction coefficient for air

effective configuration. Thus CFD simulation is effective, as it allows computation for various geometries, and study of the effect of various design configurations on heat transfer and flow characteristics.
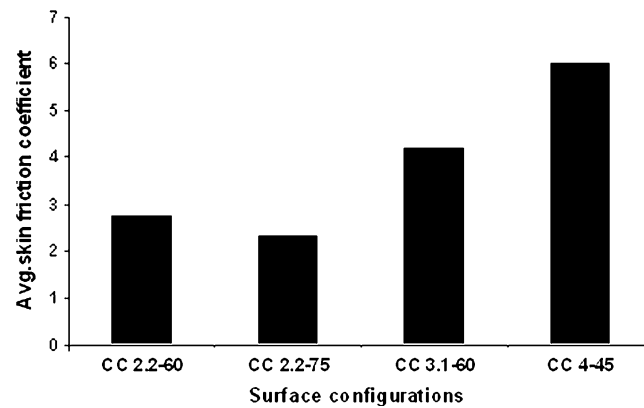

Fig. 10 Results of CFD analysis, average skin friction coefficient for argon

Table 6 Coefficients of Nu and $f*Re$ correlations

Surface	$Nu = C1 + C2$		$f*Re = C1 + C2*Re$	
	$C1$	$C2$	$C1$	$C2$
CC 2.2–60	6.2884	0.1648E-01	28.3023	0.3952E-01
CC 2.2–75	8.8088	0.2307E-01	38.7619	0.5413E-01
CC 3.1–60	5.0307	0.1817E-01	49.5291	0.6916E-01
CC 4–45	2.9241	0.7655E-02	21.3186	0.2948E-01

The results of design calculation carried out on recuperator matrix of different surfaces indicate that recuperator matrix core volume increases with the aspect ratio and decreases with the corrugation angle. Among the surfaces used for the design calculations CC 2.2–75 requires least core volume for the specified condition. However the constants in Table 6 are available through experimental studies reported by Utriainen and Sunden [3], which is required for design calculations.

The results of CFD analysis show the direct variation of aspect ratio and heat transfer coefficient and inverse variation of corrugation angle and heat transfer coefficient for a given size and given input flow variables. The surface CC 4–45 is most effective among the surface analyzed in CFD analysis for same size and same input flow variables.

The results of CFD analysis for average skin friction coefficients can be used to compare with the results of design calculations for minimum recuperator matrix volume. The cross corrugated surface with the minimum recuperator matrix volume (i.e., CC 2.2–75) is also one with the minimum average skin friction coefficient for the separating wall. Thus CFD analysis can be used to narrow down our studies on heat transfer surfaces for minimum core volume of recuperator matrix.

Appendix

The design calculations for each heat transfer surface are based on the following algorithm. Here is a simplified algorithm for primary surface configurations.
Input:

Total heat transferred in the recuperator matrix, calculated with help of specified condition.

Step 1. Choose Re number for air side. Calculate velocity, W_{air}, for air side

$$W_{air} = \frac{Re_{air} \nu_{air}}{D_{h,air}}. \tag{3}$$

Step 2. Calculate velocity of gas side from

$$W_{gas} = W_{air} \frac{\dot{m}_{gas} \rho_{air} A_{air}}{\dot{m}_{air} \rho_{gas} A_{gas}}. \tag{4}$$

Step 3. Calculate Nu numbers and f factors, for both sides, using correlations in Table 6.

Step 4. Calculate heat transfer coefficients, for both sides. Here air side

$$h_{air} = \frac{Nu_{air} k_{air}}{D_{h,air}}. \tag{5}$$

Step 5. Calculate the overall heat transfer coefficient from

$$U = \frac{1}{\left(\frac{1}{h_{air}} + \frac{1}{h_{gas}} + \frac{S}{k_{wall}} \right)}. \tag{6}$$

Step 6. Calculate the total heat transfer area:

$$A_{total} = \frac{q}{U \Delta T_{log}}. \tag{7}$$

Step 7. The coefficient of compactness C is calculated from a representative control volume of each heat transfer surface configuration:

$$C = \frac{A_{total}}{V_{recuperator}}. \tag{8}$$

Step 8. The total frontal area (flow area at inlet) is obtained from

$$A_{front} = A_{air} + A_{gas} + A_{metal}. \tag{9}$$

Step 10. The total length of the recuperator heat transfer matrix is then obtained from

$$L_{recuperator} = \frac{V_{recuperator}}{A_{front}}. \tag{10}$$

Step 11. The pressure losses for both sides. Here the air side

$$\Delta P = 2 f_{air} \frac{L_{recuperator}}{D_{h,air}} \rho_{air} W_{air}^2. \tag{11}$$

Step 12. The total relative pressure losses:

$$\Delta P_{total} = \frac{\Delta P_{air}}{p_{air}} + \frac{\Delta P_{gas}}{p_{gas}}. \tag{12}$$

Step 13. If ΔP_{total} is not equal to 0.03 then go back to step one change the Reynolds number.

References

1. McDonald CF (2000) Low cost recuperator concept for micro-turbine applications, ASME paper GT-167
2. Uechi H, Kimijima S et al (2004) Cycle analysis of gas turbine—fuel cell hybrid micro generation system. J Eng Gas Turbines Power 26:755–762
3. Utriainen E, Sunden B (2002) Evaluation of the cross corrugated and some other candidate heat transfer surfaces for micro turbine recuperators. J Eng Gas Turbines Power 124:550–560
4. Heavner RL, Kumar H et al (1993) Performance of an industrial plate heat exchanger: effect of chevron angle. In: AIChE symposium, series no. 295, vol 89, Heat transfer. American Institute of Chemical Engineering, Atlanta, pp 262–267
5. Focke WW, Zachariades J et al (1985) The effect of the corrugation inclination angle on the thermo hydraulic performance of plate heat exchangers. Int J Heat Mass Transf 28:1469–1479
6. Muley A, Manglik RM (1999) Experimental study of turbulent flow heat transfer and pressure drop in a plate heat exchanger with chevron plates. J Heat Transf 121:110–117
7. Muley A, Manglik RM (1998) Investigation of enhanced heat transfer in low Reynolds number flows in a plate heat exchanger. In: Proceedings ASME heat transfer division, vol 361–363. ASME, New York, pp 295–302
8. Stasiek J, Ciofalo M et al (1996) Investigation of flow and heat transfer in corrugated passages—I. Experimental results. Int J Heat Mass Transf 39:149–164
9. Ciofalo M, Stasiek J et al (1996) Investigation of flow and heat transfer in corrugated passages—II. Numerical simulations. Int J Heat Mass Transf 39:165–192
10. Yin J, Li G, Feng Z (2006) Effects of intersection angles on flow and heat transfer in corrugated-undulated channels with sinusoidal waves. J Heat Transf 128:819–828
11. Shah RK, Wanniarachchi AS (1991) Plate heat exchanger design theory. In: Buchlin JM (ed) Industrial heat exchangers, vol 4. van Kareman Institute Lecture Series
12. Vlasogiannis P, Karagiannis G et al (2002) Air-water two-phase flow and heat transfer in a plate heat exchanger. Int J Multiphase Flow 28:757–772
13. Lioumbas IS, Mouza AA et al (2002) Local velocities inside the gas phase in counter current two-phase flow in a narrow vertical channel. Chem Eng Res Des 80:667–673
14. Focke WW, Knibbe PG (1986) Flow visualization in parallel-plate ducts with corrugated walls. J Fluid Mech 165:73–77
15. Menter F, Esch T (2001) Elements of industrial heat transfer predictions. In: Sixteenth Brazilian congress of mechanical engineering (COBEM) 26–30 Nov 2001, Uberlandia